MULTI-PASS DIFFERENTIAL RADAR INTERFEROMETRY
WITH THE AID OF GIS

L. Ge[a], H.C. Chang[b], C. Rizos[a], J. Trinder[a]

School of Surveying and Spatial Information Systems, The University of New South Wales, Sydney, NSW 2052, Australia –
[a](l.ge, c.rizos, j.trinder)@unsw.edu.au, [b]hsing-chung.chang@student.unsw.edu.au

KEY WORDS: Satellite, radar, SAR, Interferometer, GIS, Monitoring

ABSTRACT:

Differential interferometric synthetic aperture radar (DInSAR) has been increasingly used to monitor ground surface deformations due to such occurrences as underground mining, fluid extraction, earthquake and volcanic activities. However, temporal decorrelation has made it difficult to derive useful information from a single pair of repeat-pass satellite radar images for vegetated regions when the time span between image acquisitions is long. A methodology is proposed for monitoring ground deformation using multi-pass differential radar interferometry (MPDInSAR) with the aid of a Geographic Information System (GIS). In this approach, several radar images covering the same region from multiple satellite passes are grouped into master-slave pairs of short temporal baselines. These image pairs are processed individually by using spaceborne repeat-pass DInSAR to generate the results depicting ground deformation, which are then exported to the GIS. These displacement images are precisely geo-referenced, reclassified and combined using various GIS tools to produce a total displacement image over the entire period of time spanned by the multiple satellite passes. The MPDInSAR approach has been tested at the underground coal mining areas in eastern Australia. Ground subsidence due to mining has been monitored using L-band JERS-1 satellite images. The RMS errors of less than 1.5 centimetre has been demonstrated.

1. INTRODUCTION

Differential interferometric synthetic aperture radar (DInSAR) has been increasingly used to monitor ground surface deformations due to such occurrences as underground mining, fluid extraction, earthquake and volcanic activities. Some studies in the UK (Wright and Stow, 1997; Wright and Stow, 1999), France (Carnec et al., 1996; Carnec and Delacourt, 2000) and Germany (Wegmuller et al., 2000; Spreckels et al., 2001) have demonstrated the capability of DInSAR for monitoring surface deformation caused by underground coal mining. The ERS-1/2 satellite images were primarily used in those studies and the results showed that the phase ambiguity becomes difficult to be resolved due to the strong phase noise caused by unfavourable vegetated cover and/or high gradient of phase fringes for long time span between the interferometric image pairs.

Underground mining subsidence normally has a magnitude of tens of centimetres over a short period of time and causes high gradient of phase fringes in its radar interferometry results. It is very difficult to resolve the ambiguity caused by dense and rapid phase change if the ground surface displacement is needed to be measured.

In this paper a methodology is proposed for monitoring ground deformation using multi-pass differential radar interferometry (MPDInSAR) with the aid of a geographic information system (GIS). This approach uses several DInSAR results with the minimal repeat cycles to accumulate the total ground surface displacement occurring over the long time span. GIS is exploited to calculate the MPDInSAR result and also to interpret and validate the results.

This approach has been tested at 2 underground coal-mines in eastern Australia. Several radar images covering the same region from multiple satellite passes are grouped and processed individually to generate DInSAR results which will be imported into GIS to form the total surface displacement as the result of MPDInSAR over the entire period of time spanned by the multiple satellite passes.

2. DIFFERENTIAL INSAR

Spaceborne repeat-pass DInSAR was used to measure the mining subsidence over short (1~2) satellite repeat cycles. Several ERS-1/2 and JERS-1 images were tested for coherence over the test sites. The test sites were more problematic with ERS-1/2 interferometric pairs because of the agricultural and forest cover resulting a lack of coherence. As a result, three JERS-1 images were chosen by considering the quality of DInSAR results and for the purpose to demonstrate the feasibility of MPDInSAR. Three interferometric pairs were formed as shown in Table 1. These interferometric pairs were processed individually to generate DInSAR results depicting ground deformation.

Pair	Master	Slave	B⊥ (m)	Time

No.				span (days)
a	08/03/95	21/04/95	94	44
b	21/04/95	04/06/95	482	44
c	08/03/95	04/06/95	557	88

Table 1. Summary of the JERS-1 interferometric pairs.

SAR image records both the amplitude and phase of the backscattered signal from the objects on the ground. The phase difference or so-called interferogram is generated by complex conjugate multiplication of the interferometric image pair. As shown in equation (1), the phase change f in interferogram is the composite of topographic information, surface displacement between the two acquisitions, atmospheric delay and noise.

$$f = f_{topo} + f_{disp} + f_{delay} + f_{noise} \qquad (1)$$

where: f_{topo} = topographic phase

f_{disp} = ground surface displacement

f_{delay} = atmospheric delay

f_{noise} = phase noise

DInSAR is the process to utilise the phase component caused by ground surface displacement and eliminate or minimise the effects due to others.

The atmospheric component is due to fluctuations of the water content in the atmosphere between the satellite and the target. The atmospheric delay can be identified using the fact that its fringe structure is independent over several interferograms (Massonnet and Feigl,, 1995) or can be modelled by using GPS network (Ge et al., 2003). In this study, the surface displacement induced by underground mining is expected to have higher spatial frequencies than the lower frequencies caused by atmospheric delay. Therefore it is reasonable to assume that the atmospheric delay can be ignored, insignificant and hence the phase changes located above the extraction sites consist exclusively of subsidence (Carnec et al., 1996).

The contribution of the topographic phase is carefully removed by using an external 1 arc second photogrammetric DEM. The resulted interferograms after removing the topographic phase are shown in Figure 1 and 2 for the two collieries.

Longwall mining technique is employed at both collieries being studied. The location of the detected subsidence as it moves along with the corresponding current mining face has been validated by the mine plan. Longwall mining leads to a typical feature of concentric circular or elliptical subsidence phase fringes (Wright and Stow, 1997).

The height ambiguity for the displacement phase is given by equation (2). A complete 2p phase change is therefore equivalent to a height displacement of ?/2 in the range direction (for JERS-1, ? / 2 = 11.75 cm).
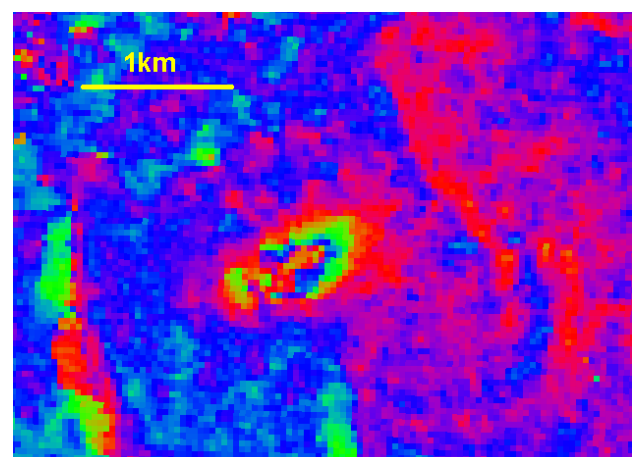
$$f_{disp} = -\frac{4p}{l} dR \qquad (2)$$

where f_{disp} = ground surface deformation component
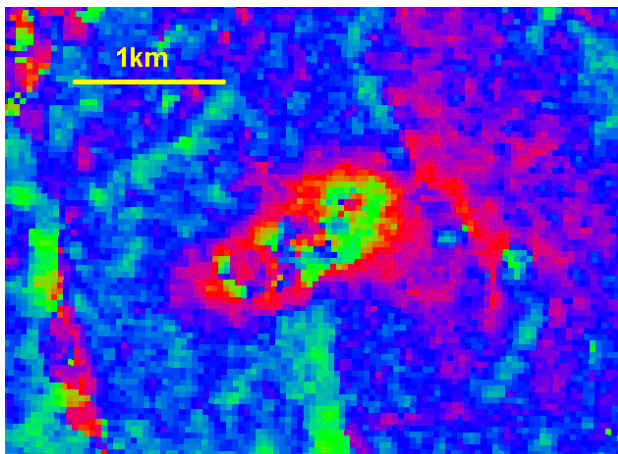
dR = height displacement in range direction

The measured phases in the interferogram are wrapped in modulo of 2p. The height displacement map can be derived by phase unwrapping the interferogram. The results are analysed and discussed in more details in section 5.
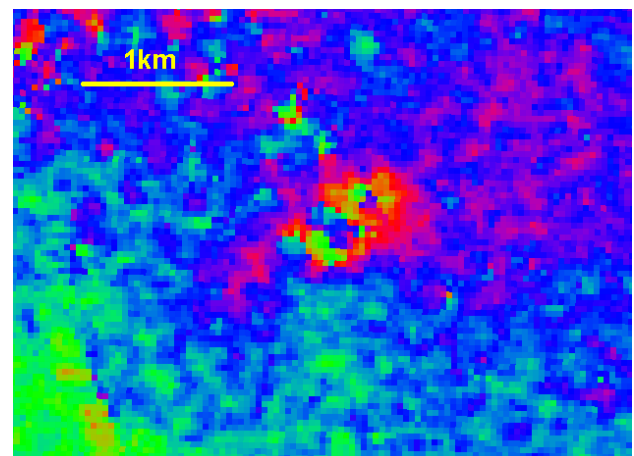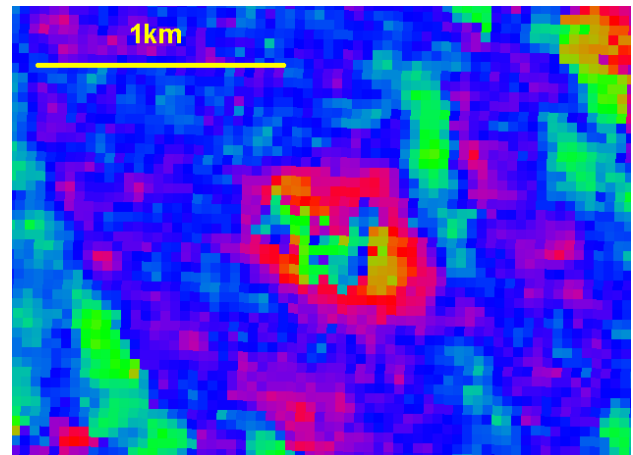

(a)

(b)

(c)

Figure 1. DInSAR interferogram at colliery A for the period of (a) 08/03/95 ~ 21/04/95, (b) 21/04/95 ~ 04/06/95 and (c) 08/03/95 ~ 04/06/95.


(c)

Figure 2. DInSAR interferogram at colliery B for the period of (a) 08/03/95 ~ 21/04/95, (b) 21/04/95 ~ 04/06/95 and (c) 08/03/95 ~ 04/06/95.

(a)

(b)

## 3. BENEFITS OF DINSAR WITH SHORT TIME INTERVAL

Although it is well known that temporal decorrelation degrades the capability of repeat-pass DInSAR, the benefits of DInSAR with short time interval (i.e., temporal baseline) can be best appreciated by comparing ERS tandem DInSAR, with a temporal baseline of only one day, to repeat-pass DInSAR with data collected by the same sensor aboard the same platform.

Data from the ERS-1/2 tandem mission have been widely used to generate digital elevation models because of the short (24 hour) time interval (temporal baseline) between the two acquisitions, which typically results in high coherence in InSAR data processing. Differential InSAR analysis based on ERS tandem data (tandem differential InSAR) has also been used to study atmospheric effects in InSAR results. In this case, the topographic contribution is carefully removed from the interferogram and an assumption is made that there is no significant ground displacement within 24 hours. What is assumed left in the differential InSAR result are atmospheric disturbances. The assumption is not valid, however, in a shallow underground mining region shown in Figure 3. The two radar images were acquired on 29 and 30 October 1995 respectively by ERS-1 and ERS-2. This tandem differential InSAR analysis has probably for the first time revealed almost 1cm subsidence in 24 hours. The mining progress from underground survey is indicated in yellow within the mine longwall. *Further profile analysis in Figure 4 shows that the resolution of the technique is about +/- 2 mm.*

In contrast to tandem differential InSAR, repeat-pass differential InSAR has been widely used to map ground surface
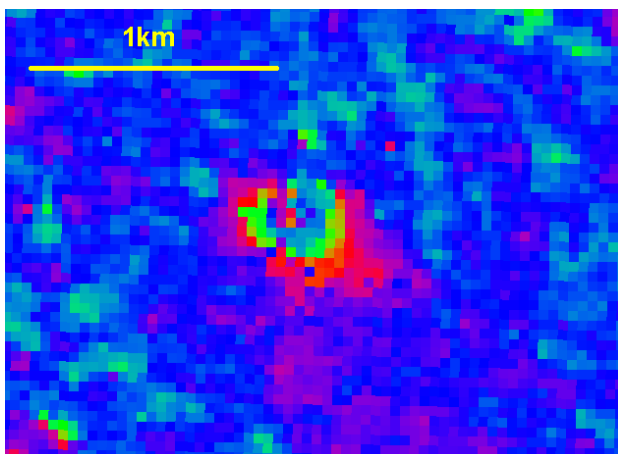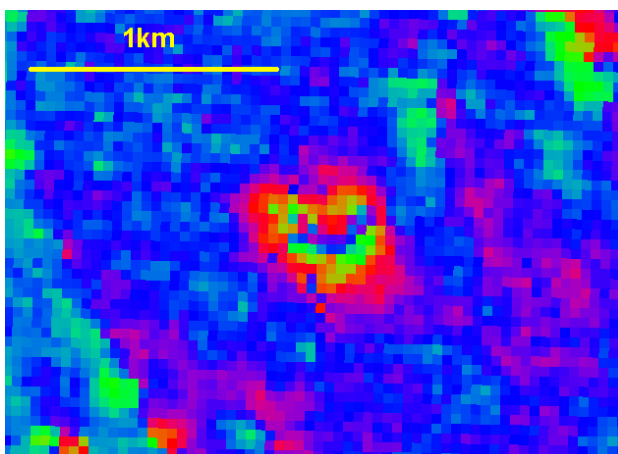
movements due to many natural (e.g., earthquakes and volcanoes) and man-made (e.g., underground mining and oil / water / gas extraction) activities. In repeat-pass differential InSAR, the master and slave images are acquired by the same sensor aboard the same platform. Therefore, the temporal baselines are multiples of 24, 35, and 44 days for Radarsat-1, ERS-1 and -2, and JERS-1, respectively, which are significantly longer than the tandem case. These much larger temporal baselines lead to temporal de-correlation which degrades the InSAR results. For example, for the same region mentioned above was monitored using two JERS-1 radar images acquired 44 days apart (i.e. 26 September 1993 and 9 November 1993) while the ground survey were carried out on three days in August, September and November 1993. Figure 5 gives a comparison between the InSAR derived profile and ground survey. It can be seen the remote sensing result agrees very well with the ground survey. *The accuracy of InSAR measured subsidence is +/- 1.4 cm from the JERS-1 repeat-pass differential InSAR, when compared to ground truth.* It has been shown, however, that repeat-pass DInSAR does have difficulty in tracking subsidence in the centre of the affected zone because the fringes are too dense. In other words, the DInSAR signal has become "*saturated*". As a result, subsidence measured by DInSAR is significantly less than ground survey (more than 5cm in this example). Unless the overburden is collapsed, it is very unlikely that mine subsidence would saturate the tandem DInSAR signal.
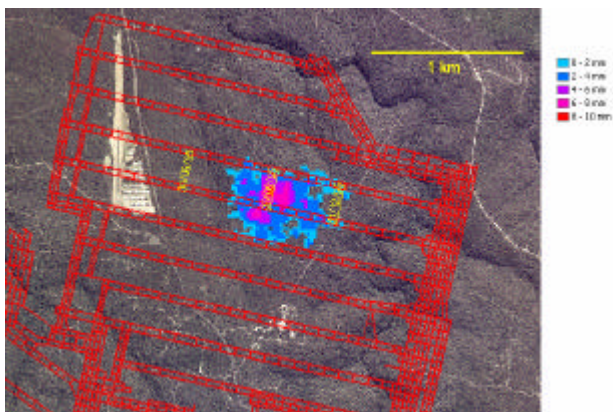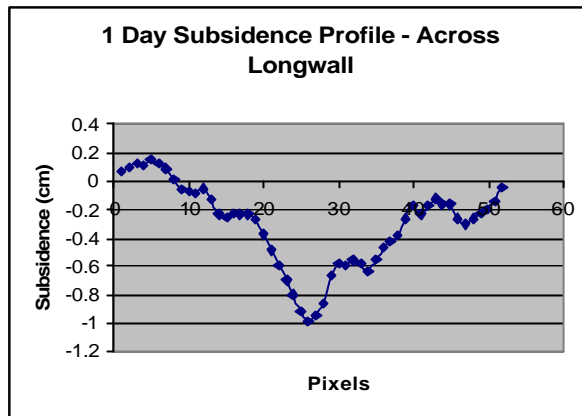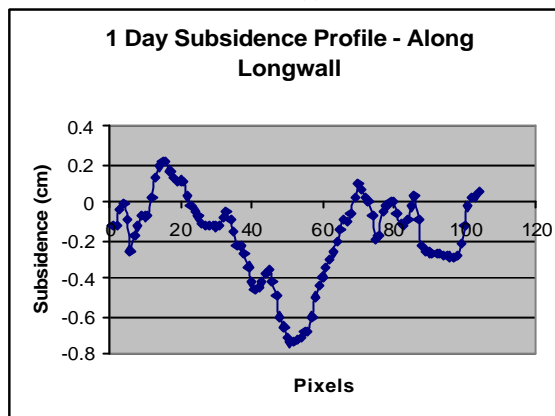

Figure 3 Contour map derived from ERS tandem DInSAR showing mine subsidence overlaid on mine plan and aerial photo.

(a)

(b)

Figure 4. Profiles derived from DInSAR result of Figure 3, showing subsidence in directions (a) across and (b) along the longwall.
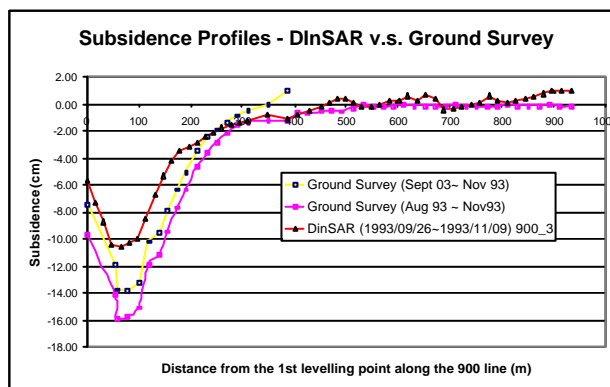

Figure 5. Comparison between repeat-pass DInSAR derived profile and ground survey.

Comparing tandem DInSAR to repeat-pass DInSAR it can be seen that due to the much shorter temporal baseline, tandem differential InSAR can measure ground displacement at a much higher resolution (2 mm vs 1.4 cm) without the problem of saturation. Although the ERS-1/2 tandem mission has become a history of success, the above comparison does highlight the benefits of DInSAR with short temporal baseline and thus the advantages of MPDInSAR. In addition, constellations of InSAR

satellites are planned for the next 5 to 10 years (Solomon et al, 2003; China Daily, 2003). Data from such future tandem missions will dramatically enhance the capability of differential InSAR through the use of MPDInSAR, which has the potential to revolutionise ground deformation monitoring.

4. MULTI-PASS DIFFERENTIAL RADAR INTEROMETRY WITH THE AID OF GIS

GIS is a method to visualise, manipulate, analyse and display data collected from many sources. A multi-pass differential radar interferometry with the aid of GIS is proposed to measure the ground surface displacement (e.g. underground mining subsidence) over a long time span. MPDInSAR uses the DInSAR results with the minimal repeat cycles to accumulate the total surface displacement over the entire time span. Therefore GIS is utilised here as an essential tool for deriving the results of MPDInSAR and also for data interpretation and validation. The height change maps derived by DInSAR are imported to GIS and analysed together with other data such as aerial photograph, mine plan and ground surveying data. The flow chart of MPDInSAR is illustrated in Figure 6.
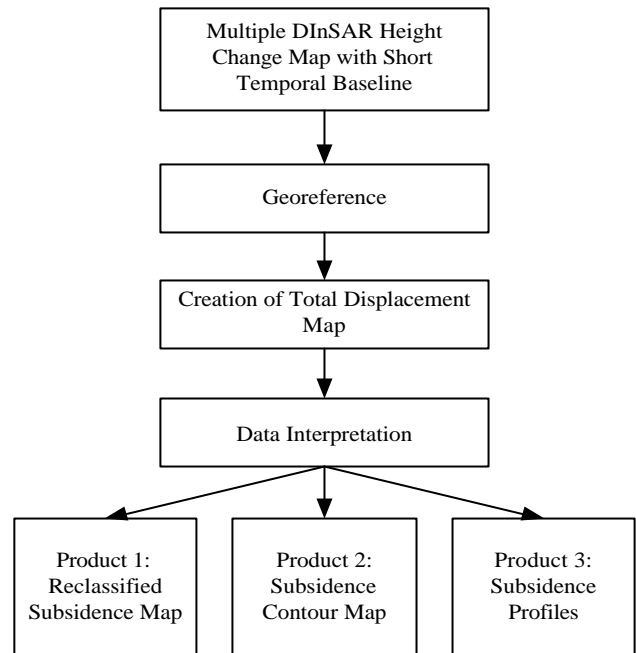
Each of the DInSAR height displacement map is precisely georeferenced, after which the total displacement map over the entire period of time spanned by the multiple satellite passes can be calculated by summing the individual displacement maps.

The subsidence maps are further interpreted against the aerial photograph and the mine plans so that the location of the subsidence can be validated.

Due to legal requirement for minimising the impact of mine-induced subsidence on ecosystem, private or public properties and facilities, mine subsidence needs to be carefully monitored on a regular basis. The location and amplitude of the subsidence are the two major concerns. With the aid of GIS, a better visual illustration of the affected subsidence areas can be generated by reclassifying the height change maps so that the non-subsiding regions are masked out and not displayed. The reclassified subsidence maps, which are the result of MPDInSAR, with the background of a local aerial photograph are shown in Figure 7. The results show a strong linkage between the local area and the subsiding area detected by MPDInSAR.

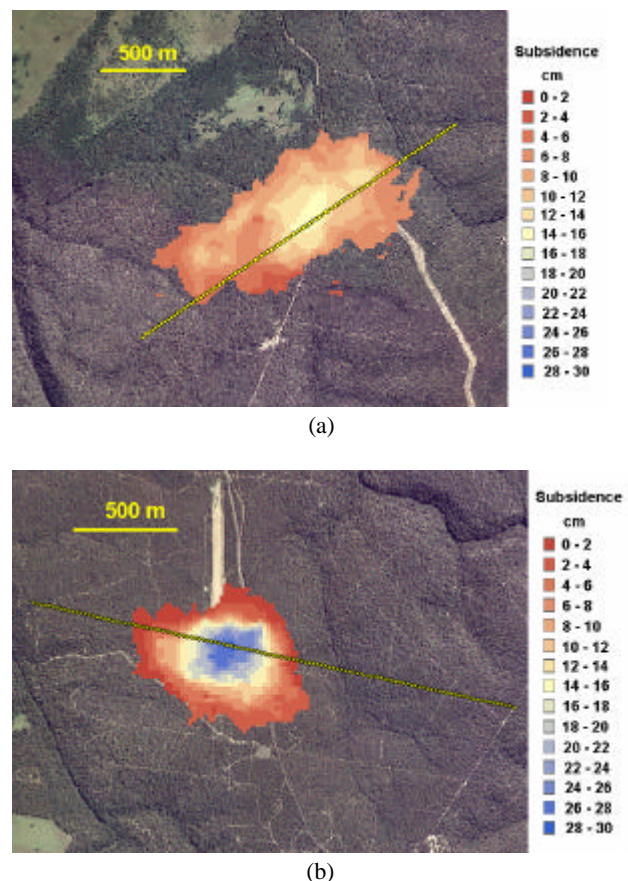Figure 6. Flow chart of MPDInSAR.

(a)

(b)

Figure 7. The reclassified subsidence maps of MPDInSAR at (a) colliery A and (b) colliery B for the period of 08/03/95 ~ 04/06/95 with the arbitrary profile lines.

5. RESULTS

To demonstrate the advantage of MPDInSAR against traditional DInSAR, the subsidence profiles of the three DInSAR pairs and also the MPDInSAR drawn along the profile lines indicated in Figure 7 are shown in Figure 8.

The maximum subsiding area moves correspondingly with the mining faces as shown from the profiles drawn from DInSAR03_04 and DInSAR04_06. Comparing the profile of MPDInSAR against the one derived from the DInSAR03_06 shows clearly that the two profiles have very similar values at the outer region of the subsidence. Near the centre of the affected zone, an extra 7 cm and 10 cm subsidence are measured by MPDInSAR at collieries A and B respectively, which could well be the case considering the result given in Figure 5.

Due to the lack of the historical ground survey data over the similar period at both mines, quantitative validation is not possible. Nevertheless, the variation of the height displacement values over the region having no expected subsidence as shown in the red rectangle in Figure 8 (b) gives an indication of the resolution. The RMS errors are between 0.9 ~ 1.5 cm.
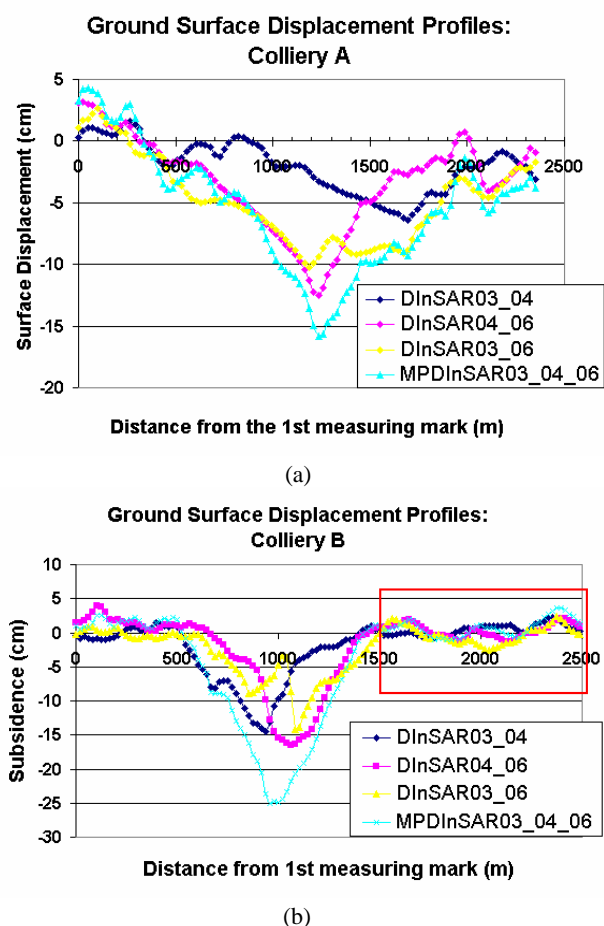

(a)

(b)

Figure 8. The subsidence profiles comparison between traditional DInSAR and MPDInSAR for (a) colliery A and (b) colliery B.

The ground surveying data acquired during the different time interval rather than the periods shown in Figure 8 is provided here as an indication of the expected amplitude of subsidence

over a certain period. The subsidence occurred at colliery A from 18 January 1995 to 10 August 1995, which is 204 days or approximately 4.6 repeat cycles of JERS-1 satellite, has a maximum subsidence of 67 cm. The subsidence occurred at colliery B from 7 July 1993 to 8 October 1993, which is 93 days or approximately 2.1 repeat cycles of JERS-1, has a maximum subsidence of 45 cm. The amplitude of subsidence depends on many variables such as mining depths and local geological structures. Therefore, the quantitative validation cannot be performed without both spatial and temporal overlaps between the interferometric results and ground surveying data.

However, if a subsidence with the vertical displacement of 40 cm vertical displacement did occur during a period of 90 days, then conventional DInSAR process would not be able to measure such a displacement correctly as being seen from Figure 8. In a single DInSAR pair if the amount of surface displacement at the centre of the subsidence region is too large it can lead the phase fringes to be too dense to be resolved correctly during the phase unwrapping process. The possible solutions are to have shorter satellite re-visit cycle or use a longer wavelength signal such as P-band. When continuous DInSAR pairs are available, the MPDInSAR can be used to measure the total surface displacement over the entire period for the case where large ground movement are expected.

The subsidence contour map derived from the results of MPDInSAR as the final demonstration of the strength of GIS is shown in Figure 9.
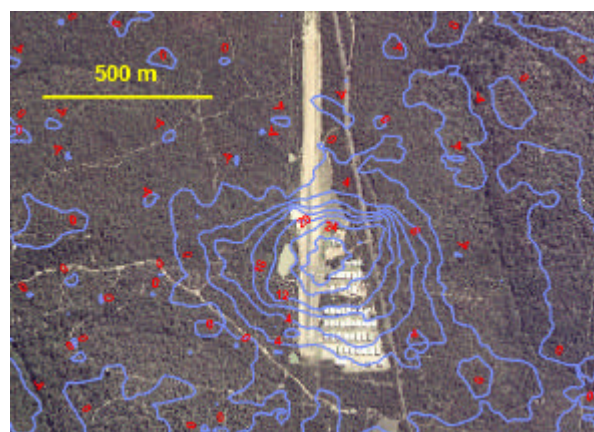

Figure 9. The subsidence contour map at colliery B derived from MPDInSAR result.

6. CONCLUSION

Underground mining subsidence normally has a magnitude of tens of centimetres over a short period of time. With this amount of ground surface displacement the phase ambiguity in the interferogram of DInSAR process is very difficult to be resolved correctly. In the multi-pass differential InSAR (MPDInSAR) method described in this paper, a series of DInSAR pairs with short (1~2) satellite repeat cycles taken over a long time span period, have been used to accumulate the

effects over the long time span. The approach provides a more accurate measurement of large subsidences, such as mine induced subsidence. This paper has also demonstrated that the results of ground surface displacement can be further interpreted and validated against other data sources with the aid of GIS. The subsidence profiles show that the derived displacements have the RMS errors of less than 1.5 cm at the non-subsiding regions.

ACKNOWLEDGMENT

REFERENCES

Carnec, C. and C. Delacourt, 2000. "Three years of mining subsidence monitored by SAR interferometry, near Gardanne, France." Journal of Applied Geophysics 43(1): 43-54.

Carnec, C., D. Massonnet, et al., 1996. "Two examples of the use of SAR interferometry on displacement fields of small spatial extent." Geophysical Research Letters 23(24): 3579-3582.

China Daily, 2003. China to build satellite group in space, http://www1.chinadaily.com.cn/en/doc/2003-11/10/content_280275.htm, 2003.

Ge, L., Chang, H.C., Janssen, V., & Rizos, C., 2003. The integration of GPS, radar interferometry and GIS for ground deformation monitoring. 2003 Int. Symp. on GPS/GNSS, Tokyo, Japan, 15-18 November, 465-472.

Massonnet, D. and K. L. Feigl, 1995. "Discrimination of geophysical phenomena in satellite radar interferograms." Geophysical Research Letters 22(12): 1537~1540.

Solomon, S.C., et al, 2003. Plan for Living on a Restless Planet Sets NASA's Solid Earth Agenda, EOS Transactions, American Geophysical Union, Vol. 84, No. 45, P485&491.

Spreckels, V., U. Wegmuller, et al., 2001. Detection and observation of underground coal mining-induced surface deformation with differential SAR interferometry. ISPRS Workshop "High Resolution Mapping from Space 2001", Institut fur Photogrammetrie and GeoInformation, Universitat Hannover.

Wegmuller, U., T. Strozzi, et al., 2000. Monitoring of mining-induced surface deformation in the Ruhrgebiet (Germany) with SAR interferometry. Geoscience and Remote Sensing Symposium, 2000. Proceedings. IGARSS 2000. IEEE 2000 International.

Wright, P. and R. Stow, 1999. "Detecting mining subsidence from space." International Journal of Remote Sensing 20(6): 1183-1188.

Wright, P. A. and R. J. Stow, 1997. Detection and measurement of mining subsidence by SAR interferometry. IEE Colloquium on Radar Interferometry (Digest No: 1997/153).